Modeling of Couplings Between Double-Ridge Waveguide and Dielectric-Loaded Resonator

Chi Wang, *Senior Member, IEEE,* and Kawthar A. Zaki, *Fellow, IEEE*

***Abstract*— Full-wave modeling of the coupling structure between a double-ridge waveguide and dielectric-loaded resonator in a rectangular cavity through an iris is presented. Eigen modes of the double-ridge waveguide, and the discontinuities of the structures are obtained by rigorous mode-matching method. By applying the cascading procedure, the reflection coefficients of the coupling structure can be obtained. From the phase variation of the reflection coefficient and circuit theory, resonant frequency and input/output coupling of the structure are accurately determined. An equivalent circuit model of the resonant structure is established. The computed results are compared with those obtained by other methods and shown to be in good agreement, which verify the theory.**

***Index Terms*— Couplings, dielectric resonators, filters, ridge waveguides.**

I. Introduction

DIELECTRIC-LOADED resonator (DR) filters are widely used in communication systems and other microwave applications because of their excellent characteristics, such as small size, low loss, and high temperature stability. If an empty rectangular waveguide is used as the input/output transmission medium, the size of the structure becomes too bulky. A ridge waveguide has lower cutoff frequency and wider bandwidth, therefore, it can be used to significantly reduce the size of the input/output waveguide and in wide band applications [1]–[5].

Accurate computation of the input/output coupling and its loading effect on the resonant frequency of the first/last stage resonator is very important for the design of high performance cavity filters. In addition, an equivalent circuit of the structure helps to understand and predict the performance of the microwave filters. Since the resonator enclosure is usually beyond cutoff at the filters passband, conventional theory cannot be applied to obtain the coupling coefficients from the transmission parameters of the two-port network. The input/output couplings are usually determined by experiment [6] or by an approximate method [14] which is neither efficient nor accurate enough for filter design. Accurate modeling of the coupling structure is, therefore, essential for the determination of the input/output coupling, loading effects on the resonant frequency, and equivalent circuit of the DR structure.

In this paper, the full-wave mode-matching method is used to model the coupling structure between the double-ridge waveguide and dielectric-loaded cavity. Eigenmodes of the double-ridge waveguide are obtained. The generalized scattering matrices of the double-ridge waveguide junction to rectangular waveguide and the dielectric resonator in rectangular waveguide discontinuities are obtained by rigorous mode-matching method. Equivalent circuit of the coupling structure is established. All the parameters of the equivalent circuit are determined from the reflection coefficient of the structure. The computed results are compared with results from the finite-element method and are shown to be in good agreement.

Manuscript received March 24, 1998; revised August 28, 1998.

C. Wang is with Celwave, Division of Radio Frequency System Inc., Marlboro, NJ 07746 USA.

K. A. Zaki is with the Department of Electrical Engineering, University of Maryland, College Park, MD 20742 USA.

Publisher Item Identifier S 0018-9480(98)09225-4.

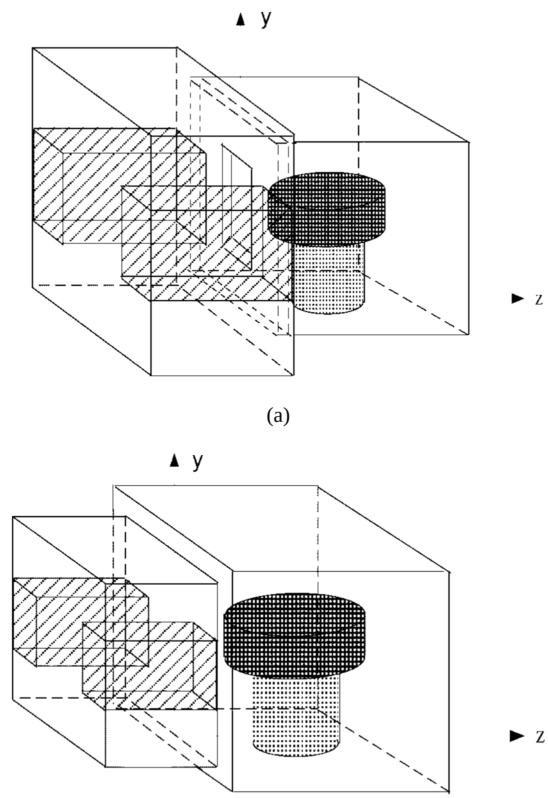

(a)

(b)

Fig. 1. Configuration of a coupling structure from a double-ridge waveguide to dielectric resonator. (a) Coupled through an iris. (b) Coupled through space.

II. Configuration and Analysis

The configurations of the coupling structure between the double-ridge waveguide and the dielectric-loaded resonator under consideration are shown in Fig. 1. In Fig. 1(a) the coupling is achieved through a slot; and in Fig. 1(b) through

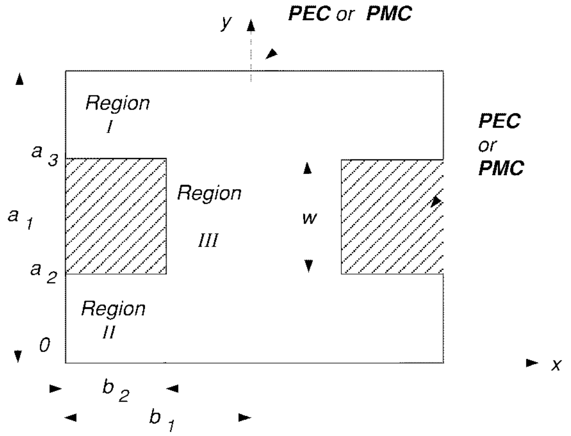

Fig. 2. Cross section of the double-ridge waveguide.

the direct connection between the double-ridge waveguide and the resonator's enclosure. To effectively couple the ridge waveguide to the DR operating in TE_{01} or HE_{11} mode by the y-component of the magnetic field, the ridges of the double-ridge waveguide have to be at the sides of the DR cavity as shown.

A. Modes and Discontinuity of the Double-Ridge Waveguide

The configuration of the double-ridge waveguide is illustrated in Fig. 2. The double-ridge waveguide has height a_1, width $2b_1$, with ridges of width w and thickness b_2. The plane at $x = 0$ at the middle of the ridge waveguide is a symmetry plane. By putting a perfect electric conductor (PEC) or a perfect magnetic conductor (PMC) at this symmetrical plane, only half of the structure needs to be considered. When the ridge waveguide is also symmetrical about $y = a_1/2$ plane, even and odd modes can be determined separately by putting PEC or PMC at that symmetry plane.

A half double-ridge waveguide is divided into three regions, region I $(-b_1 \le x \le b_2 - b_1, a_3 \le y \le a_1)$, II $(-b_1 \le x \le b_2 - b_1, 0 \le y \le a_2)$, and III $(b_2 - b_1 \le x \le 0, 0 \le y \le a_1)$, as shown in Fig. 2. The longitudinal (z directed) fields of the ridge waveguide eigenmodes are expanded in normal TE and TM modes in each region, which satisfies the wave equation

$$\nabla_t^2 \, E_z + k_c^2 E_z = 0 \tag{1}$$

or

$$\nabla_t^2 H_z + k_c^2 H_z = 0. \tag{2}$$

The transverse fields can be expressed in terms of the normal field components H_z for TE mode and E_z for TM modes as

$$\vec{H}_t^h = -\frac{\gamma^h}{k_c^{2h}} \, \nabla_t H_z^h \tag{3}$$

$$\vec{E}_t^h = \frac{j\omega\mu}{k_c^{2h}} \, \hat{z} \times \nabla_t H_z^h \tag{4}$$

$$\vec{H}_t^e = -\frac{j\omega\epsilon}{k_c^{2e}} \, \hat{z} \times \nabla_t E_z^e \tag{5}$$

$$\vec{E}_t^e = -\frac{\gamma^e}{k_c^{2e}} \, \nabla_t E_z^e. \tag{6}$$

The boundary conditions require that the tangential electric and magnetic fields at the interfaces of regions I–III to be continuous as

$$\vec{E}_t^{p\mathrm{III}}(x,y) = \begin{cases} \vec{E}_t^{p\mathrm{I}}(x,y)_{x=b_1-b_2}, & a_3 \le y \le a_1 \\ 0, & a_2 \le y \le a_3 \\ \vec{E}_t^{p\mathrm{II}}(x,y)_{x=b_1-b_2}, & 0 \le y \le a_2 \end{cases} \tag{7}$$

$$\vec{H}_t^{p\mathrm{III}}(x,y) = \begin{cases} \vec{H}_t^{p\mathrm{I}}(x,y)_{x=b_1-b_2}, & a_3 \le y \le a_1 \\ \hat{n} \times \vec{J}_s, & a_2 \le y \le a_3 \\ \vec{H}_t^{p\mathrm{II}}(x,y)_{x=b_1-b_2}, & 0 \le y \le a_2 \end{cases} \tag{8}$$

$$p = h \text{ or } e$$

by taking proper inner product, a characteristic equation for the cutoff wavenumber of the ridge waveguide can be obtained. Searching for the zero determinant of the equation, the cutoff wavenumber k_c of the double-ridge waveguide can be obtained [5], [15]. All the field coefficients of the eigen modes can then be obtained by solving the equation.

Full-wave mode-matching technique is used to obtain the generalized scattering matrices of the discontinuities from the double-ridge waveguide with ridges at left and right sides of the enclosure to empty waveguide (iris and cavity). Using the modeling method described in [16] from the boundary condition equations on the interface of the discontinuity, taking proper inner product and performing some matrix operation, the desired generalized scattering matrix $[S]$ of the discontinuity can be obtained.

B. Modeling of the Coupling Structure Between Double-Ridge Waveguide and DR Cavity

The modeling procedure described in [12] is used to obtain the generalized scattering matrices of the dielectric-loaded resonator in a rectangular waveguide. Applying the mode-matching procedure at the artificial boundary at $r = a$ as [12], [13] by using the Bessel–Fourier series [10]–[13], the fields in the cylindrical region can be related to the fields in the waveguide regions. The generalized scattering matrix of the dielectric-loaded resonator in a rectangular waveguide can then be obtained.

Knowing the generalized scattering matrices of all the discontinuities, the whole structure can be analyzed using the cascading procedure [7], [8]. Fig. 3 shows the configuration and the network representation of a double-ridge waveguide input/output structure coupled to a DR loaded cavity through an iris (small waveguide) and its S-matrix network representation. The cavity is formed by placing a conducting wall (PEC) at the left and right sides of the DR with distances d_{lt} and d_{rt} from the reference plane, respectively. An iris at the left side of the DR is connected to an input/output double-ridge waveguide. Cascading the equivalent S-matrices together and applying the short condition at DR cavity's right side, the reflection coefficients of the total structure can be obtained. From the phase variation of S_{11}, one can obtain the input/output coupling and the loaded resonant frequency of the DR cavity [6].

Fig. 4 shows the configuration of double-ridge waveguide input/output structure coupled to a DR loaded cavity through space and its S-matrix network representation. Similar to that of the iris coupled case, the structure can be solved by

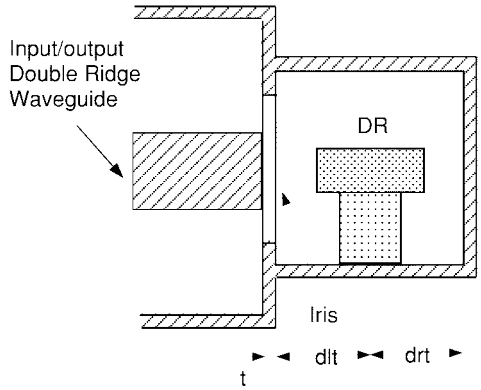

(a)

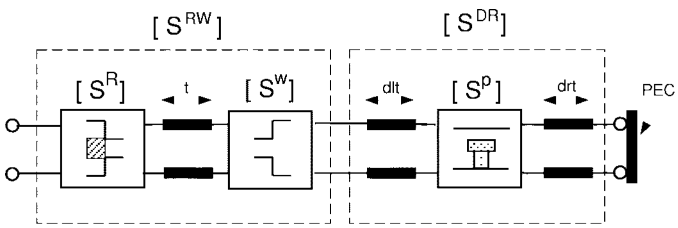

(b)

Fig. 3. (a) Configuration of a double-ridge waveguide coupled to a DR cavity through an iris. (b) S-matrix network representation of the structure.

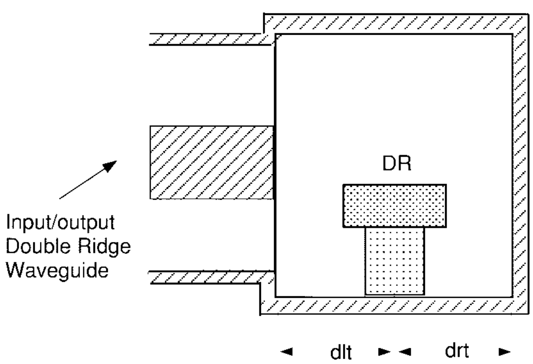

(a)

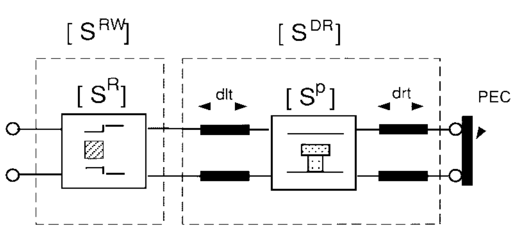

(b)

Fig. 4. (a) Configuration of a double-ridge waveguide coupled to a DR cavity through space. (b) S-matrix network representation of the structure.

cascading the scattering matrices of the double-ridge waveguide to large rectangular waveguide discontinuity with the dielectric-loaded waveguide shorted at the right side as shown in Fig. 4(b).

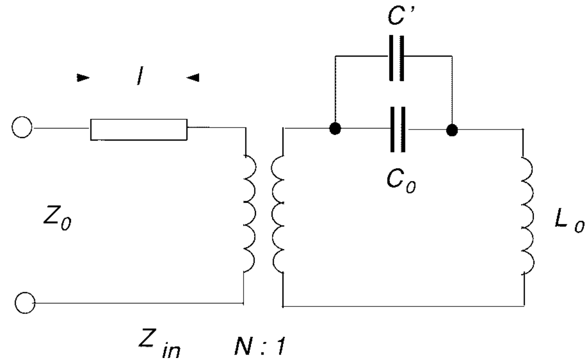

Fig. 5. Equivalent circuit of the waveguide to resonator cavity coupling structure.

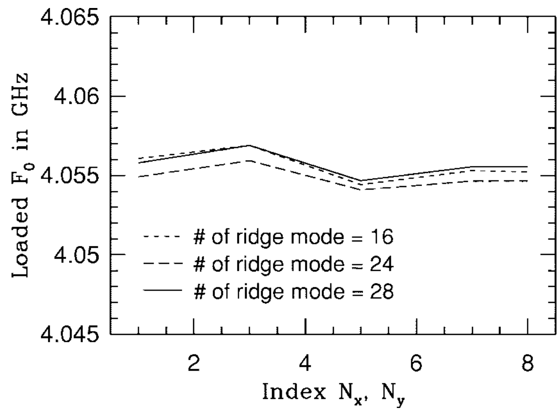

(a)

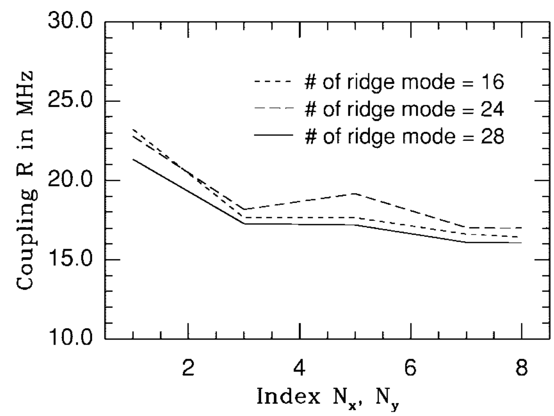

(b)

Fig. 6. Convergence of the numerical results versus number of modes in both ridge and DR waveguides. (a) Convergence of the loaded resonant frequency. (b) Convergence of the input/output coupling R.

C. Equivalent Circuit of the Coupling Structure

From the reflection coefficients of the coupling structure, an equivalent circuit can be derived to help in the design. Since the dielectric enclosure is usually a waveguide below cutoff, it is convenient to represent the DR cavity by a resonant LC circuit, as shown in Fig. 5. L_0 and C_0 have the resonant frequency of the unloaded DR cavity. C' represents the effect of the loading and discontinuities on the resonant frequency of the DR cavity. Thus the parallel combination L_0 and $C_0 + C'$ has the same resonant frequency of the whole structure. The

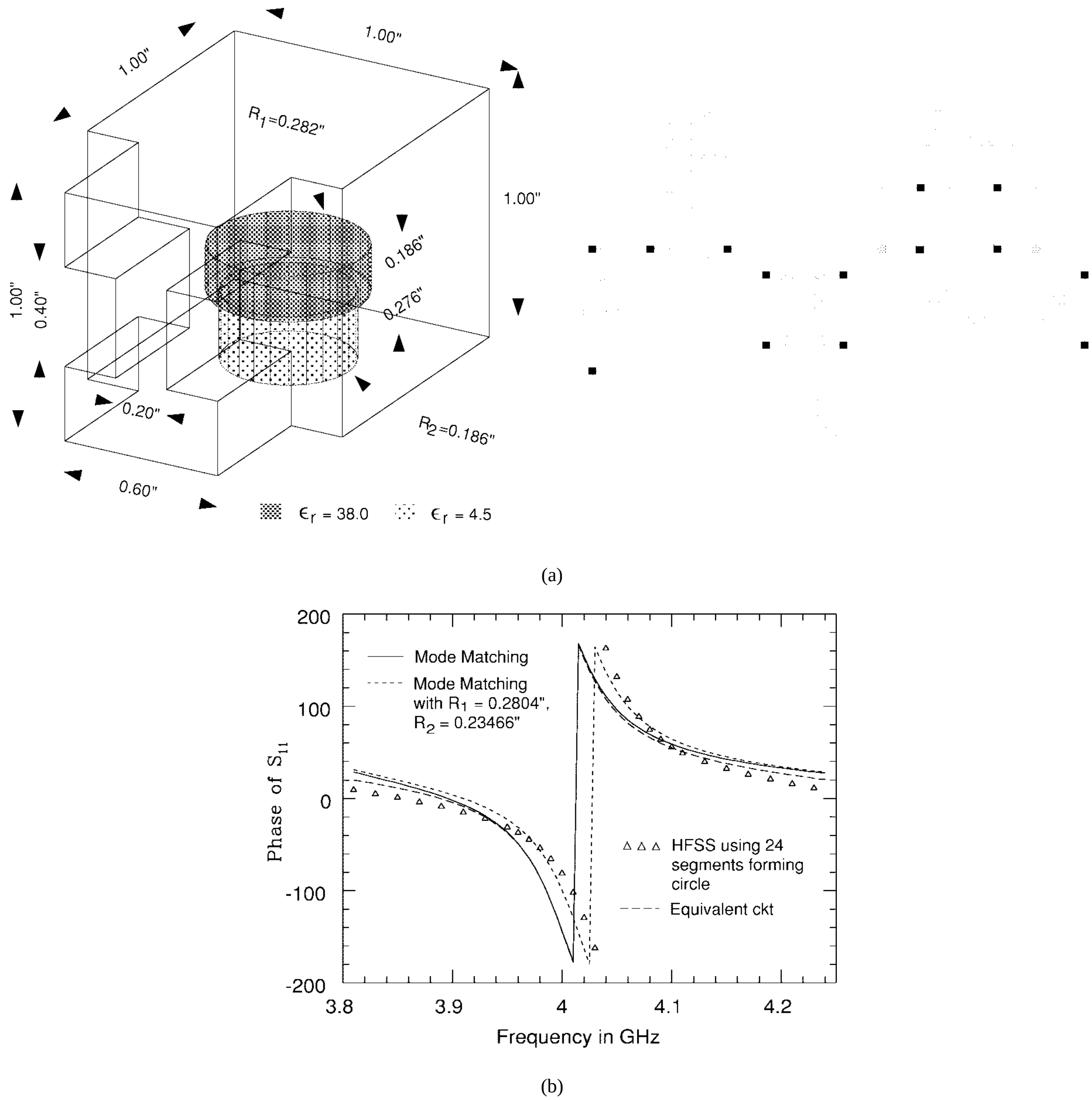

Fig. 7. (a) Configuration and the equivalent circuit of the double-ridge waveguide coupled with DR cavity via space. (b) Computed phase of the reflection coefficients.

transformer characterizes the coupling coefficient of the ridge waveguide to DR cavity. A length of transmission line l represents the phase offset introduced by the discontinuities.

It is easy to obtain the reflection coefficient of the equivalent circuit without the effect of the transmission line l as

$$\Gamma = \frac{Z_{\text{in}} - Z_0}{Z_{\text{in}} + Z_0} = \frac{N^2\left(j\omega L_0 + \dfrac{1}{j\omega C_1}\right) - Z_0}{N^2\left(j\omega L_0 + \dfrac{1}{j\omega C_1}\right) + Z_0} \tag{9}$$

let

$$N = \sqrt{\frac{Z_0}{2\pi R}} \tag{10}$$

where R is the normalized input/output coupling [6]. Then we can get

$$\Gamma = -\frac{R^2 - f^2L_0^2\left(1 - \dfrac{f_l^2}{f^2}\right)^2 - j2fL_0R\left(1 - \dfrac{f_l^2}{f^2}\right)}{R^2 + f^2L_0^2\left(1 - \dfrac{f_l^2}{f^2}\right)^2} \tag{11}$$

where f_l is the loaded resonant frequency of the coupling structure. The phase of the reflection coefficient can then be obtained as

$$\tan\theta = \frac{2f\left(\dfrac{R}{L_0}\right)\left(1 - \dfrac{f_l^2}{f^2}\right)}{f^2\left(1 - \dfrac{f_l^2}{f^2}\right)^2 - \left(\dfrac{R}{L_0}\right)^2} \approx \frac{4\left(\dfrac{R}{L_0}\right)(f - f_l)}{4(f - f_l)^2 - \left(\dfrac{R}{L_0}\right)^2} \tag{12}$$

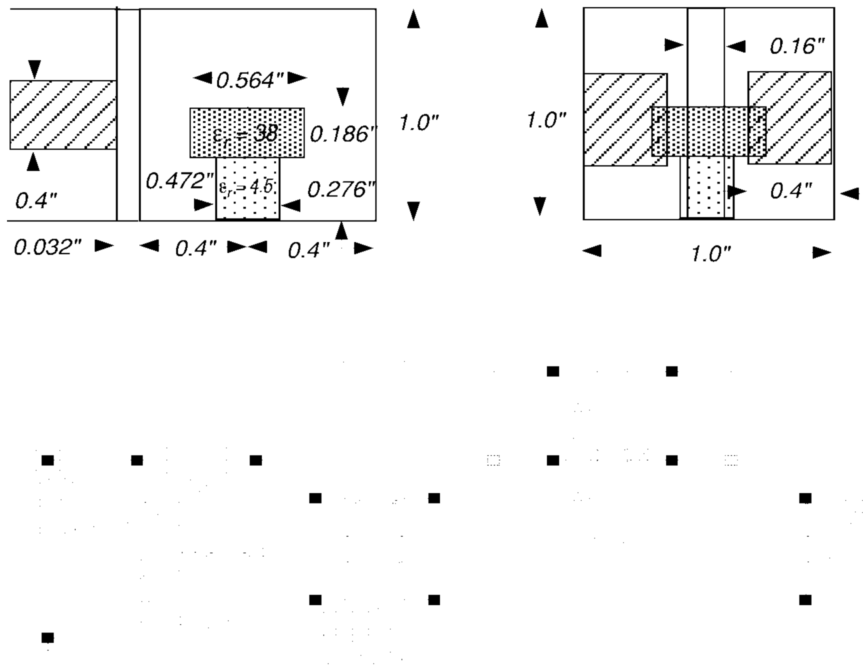

(a)

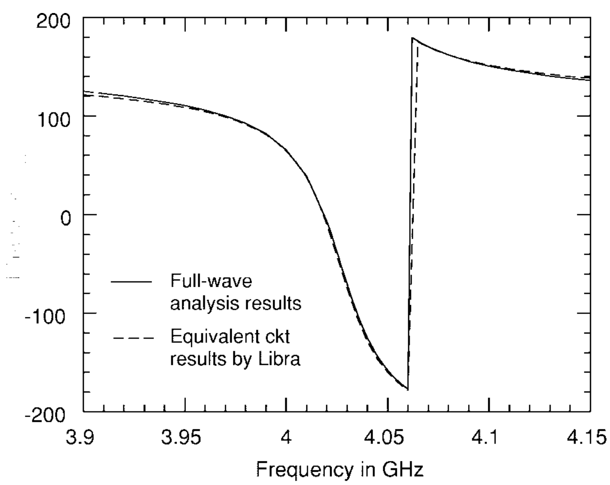

(b)

Fig. 8. (a) Configuration and the equivalent circuit of the double-ridge waveguide coupled with DR cavity via iris. (b) Computed phase of the reflection coefficients.

by letting $L_0 = 1.0$ nH, the input/output coupling coefficient R in megahertz of the resonant structure can be related to the phase change θ of the reflection coefficient at frequency f as

$$R = 2(f - f_l)\frac{1-\cos\theta}{\sin\theta}. \tag{13}$$

The external Q of the structure can be obtained as [14]

$$Q_e = \frac{f_l}{R}. \tag{14}$$

It can be shown from the equivalent circuit that $d\theta/df$ is maximum at the loaded resonant frequency f_l. Therefore, the loaded resonant frequency can be determined by searching for the peak of $d\theta/df$. The input/output coupling R can readily be computed from the phase change of a nearby frequency to the loaded resonant frequency.

III. Numerical Results

A computer program has been developed to implement the modeling method presented above. The program computes the unloaded resonant frequency of the DR cavity, loaded resonant frequency of the double-ridge waveguide to dielectric-loaded resonator in rectangular enclosure, the input/output coupling coefficient R, and the parameters of the equivalent circuit of the structure.

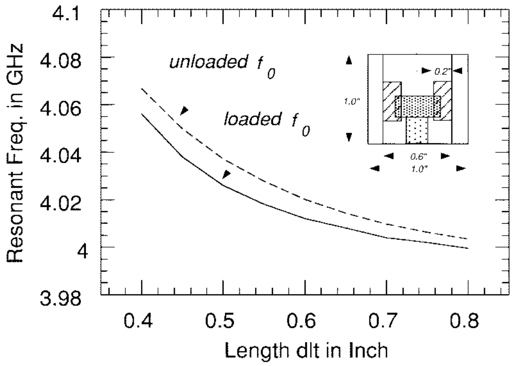

(a)

(a)

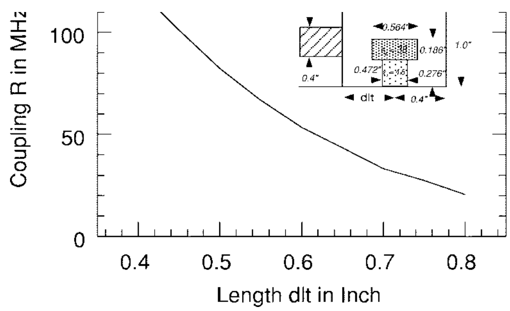

(b)

Fig. 9. (a) Unloaded and loaded resonant frequency versus the distance between ridge waveguide and DR. (b) Input/output coupling versus the distance between ridge waveguide and DR.

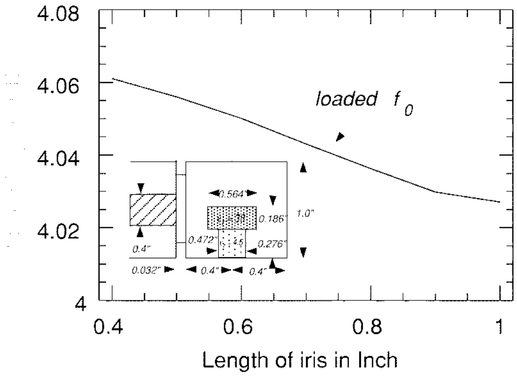

(a)

(a)

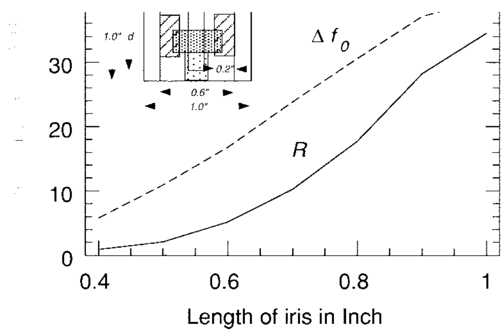

(b)

Fig. 10. (a) Loaded resonant frequency versus the length of iris. (b) Input/output coupling versus the length of iris.

From previous analysis, the coupling mechanism under consideration uses the dominant mode of double-ridge waveguide to couple the dielectric-loaded resonator in the rectangular cavity of either TE_{01} mode or HE_{11} mode by H_y field. The boundary condition at $x = 0$ plane of the modeling is, therefore, a PEC. Iris should be in the y direction, which is the same as that of the magnetic field, to achieve maximum coupling. To ensure accurate computation of both loaded resonant frequency and the input/output coupling R, convergence test is investigated. Fig. 6 presents the typical convergence of the loaded resonant frequency and the input/output coupling R versus the number of ridge waveguide modes and the modes in the dielectric-loaded waveguide in the discontinuity computation. To achieve accurate results, more than 24 ridge waveguide modes and mode index $N_x, N_y \geq 7$ of the dielectric-loaded waveguide is recommended in the frequency and coupling computation.

Fig. 7 shows the computed reflection coefficients of a double-ridge waveguide directly coupled to a dielectric-loaded resonator cavity by both the mode-matching method and the finite element method (HFSS). It is seen that the resonant frequencies of the structure obtained by two methods are close in value, and the phases of the reflection coefficients computed by the two methods are in good agreement. The figure also shows that the results obtained by the equivalent circuit are in excellent agreement with the rigorous full-wave analysis ones.

Fig. 8 gives the computed results of the coupling structure of a double-ridge waveguide to a dielectric-loaded resonator cavity via an iris 1.0 in long and 0.16 in wide by both full-wave analysis and the obtained equivalent circuit. Excellent agreement between the rigorous full-wave analysis and the equivalent circuit results has been obtained and verifies the correctness of the equivalent circuit model and its parameter computation.

Fig. 9 gives the resonant frequencies and the input/output coupling of the ridge waveguide to DR cavity versus the distance between the ridge waveguide and center of the dielectric resonator. Large input/output coupling range can be obtained by space coupled ridge waveguide and the dielectric-loaded resonator cavity. The coupling increases significantly when the waveguide is closer to the DR, and the loaded resonant frequency decreases only slightly. This is because the unloaded resonant frequency of the cavity increases and it cancels the effect of the loading on the loaded resonant frequency.

Fig. 10 shows the computed loaded resonant frequency and the input/output coupling between a double-ridge waveguide and a TE mode dielectric-loaded resonator in rectangular enclosure as function of the length of the iris. It is shown that the input/output coupling increases and the loaded resonant frequency decreases as the width of the iris increases. The decrease of the loaded resonant frequency is due to the loading

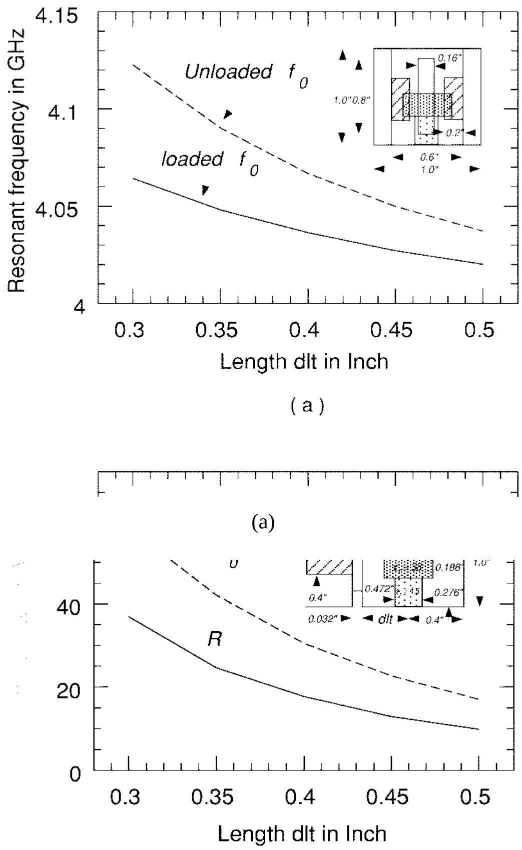

(b)

Fig. 11. (a) Unloaded and loaded resonant frequency versus the distance between iris and DR. (b) Input/output coupling versus the distance between iris and DR.

and the opening of the iris which is equivalent to increasing size of the dielectric-loaded cavity. The difference between the unloaded resonant frequency of the DR cavity and the loaded resonant frequency of the coupling system is also shown in the figure. It is seen that the difference between the two resonant frequencies Δf_0 has the same variation as the input/output coupling R and is slightly higher than the coupling. The effect of the coupling system on the resonant frequency Δf_0 is due to both the loading of the input/output coupling and the opening of the iris on the resonant frequency of the DR cavity which decreases the unloaded resonant frequency of the cavity.

As the magnetic field of the DR cavity at the side wall is not as strong as that near the dielectric resonator, the full length iris may not be able to achieve enough input/output coupling. To increase the coupling between the ridge waveguide and the DR cavity via iris, one may decrease the distance between the dielectric resonator and the coupling iris to increase the strength of the tangential magnetic field. Fig. 11 presents the resonant frequencies and the input/output coupling of the ridge waveguide to DR cavity versus the distance between the iris and the DR. It is seen that the coupling increases when the iris is closer to the dielectric resonator. When decreasing the distance, both resonant frequency and the input/output coupling of the DR cavity increases.

IV. Conclusions

Full-wave modeling of the coupling structure of the double-ridge waveguide to dielectric resonator in a rectangular waveguide through an iris and space is presented. Eigen modes of the double-ridge waveguide and the generalized scattering matrices of all the discontinuities in the structures are obtained. By using the cascading procedure, the reflection coefficients of the coupling structure are obtained. From the phase variation of the reflection coefficient and the circuit theory, loaded resonant frequency and input/output coupling of the structure including the effect of both waveguide discontinuities and dielectric-loaded resonator are accurately determined. An equivalent circuit model of the coupling structure considering all the discontinuities is established. The good agreement between the results by the present method and that by finite element method verifies the theory.

Acknowledgment

The authors would like to thank Dr. R. Mongia of ComDev Inc., Canada, for his valuable suggestions.

References

[1] S. B. Cohn, "Properties of ridge wave guide," *Proc. IRE*, vol. 35, pp. 783–789, Aug. 1947.
[2] S. Hopfer, "The design of ridged waveguide," *IRE Trans. Microwave Theory Tech.*, vol. MTT-3, pp. 20–29, Oct. 1955.
[3] J. P. Montgomery, "On the complete eigenvalue solution of ridged waveguide," *IEEE Trans. Microwave Theory Tech.*, vol. MTT-19, pp. 547–555, June 1971.
[4] Y. Utsumi, "Variational analysis of ridged waveguide," *IEEE Trans. Microwave Theory Tech.*, vol. MTT-33, pp. 111–120, Feb. 1984.
[5] R. R. Mansour, R. S. K. Tong, and R. H. Macphie, "Simplified description of the field distribution in finlines and ridge waveguides and its application to the analysis of E-plane discontinuities," *IEEE Trans. Microwave Theory Tech.*, vol. MTT-36, pp. 1825–1832, Dec. 1988.
[6] A. E. Atia and A. E. William, "Measurements of intercavity coupling," *IEEE Trans. Microwave Theory Tech.*, vol. MTT-23, pp. 519–522, June 1975.
[7] R. Mittra and J. R. Pace, "A new technique for solving a class of boundary value problems, " *IEEE Trans. Antennas Propagat.*, vol. AP-11, pp. 617, Sept. 1963.
[8] A. S. Omar and K. Schünemann, "Transmission matrix representation of finline discontinuities," *IEEE Trans. Microwave Theory Tech.*, vol. MTT-33, pp. 765–770, Sept. 1985.
[9] S.-W. Chen and K. A. Zaki, "Dielectric ring resonators loaded in waveguide and on substrate," *IEEE Trans. Microwave Theory Tech.*, vol. 39, pp. 2069–2076, Dec. 1991.
[10] R. Gesche and N. Löchel, "Scattering by a lossy dielectric cylinder in a rectangular waveguide," *IEEE Trans. Microwave Theory Tech.*, vol. MTT-36, pp. 137–144, Jan. 1988.
[11] ——, "Two cylindrical obstacles in a rectangular waveguide—resonances and filter applications," *IEEE Trans. Microwave Theory Tech.*, vol. 37, pp. 962–968, June 1989.
[12] X. P. Liang and K. A. Zaki, "Modeling of cylindrical dielectric resonators in rectangular waveguides and cavities," *IEEE Trans. Microwave Theory Tech.*, vol. 41, pp. 2174-2181, Dec. 1993.
[13] H.-W. Yao, K. A. Zaki, A. E. Atia, and R. Hershtig, "Full wave modeling of conducting posts in rectangular waveguides and its applications to slot coupled combline filters," *IEEE Trans. Microwave Theory Tech.*, vol. 43, pp. 2824–2830, Dec. 1995.
[14] G. L. Matthaei, L. Young, and E. M. T. Jones, *Microwave Filters, Impedance-Matching Networks and Coupling Structure*. New York: McGraw-Hill, 1984.
[15] H. W. Yao, A. Abdelmonem, J.-F. Liang, X.-P. Liang, K. A. Zaki, and A. Martin, "Wide band waveguide and ridge waveguide T-junctions for diplexer applications," *IEEE Trans. Microwave Theory Tech.*, vol. 41, pp. 2166–2173, Dec. 1993.
[16] H. W. Yao, A. Abdelmonem, J.-F. Liang, and K. A. Zaki, "Analysis and design of microstrip-to-waveguide transitions," *IEEE Trans. Microwave Theory Tech.*, vol. 42, pp. 2371–2380, Dec. 1994.

Chi Wang (S'95–M'97–SM'98) received the B.S. and M.S. degrees from Beijing Institute of Technology, Beijing, China, in 1983 and 1986, respectively, and the Ph.D. degree at the University of Maryland, College Park, in 1997, all in electrical engineering.

From 1986 to 1989, he was an Electrical Engineer at North China Vehicle Research Institute, Beijing, China, where he was engaged in developing an auto test system. From 1990 to 1992, he was with Beijing XYE Electronics Inc. working on RF circuit and system design. He spent one year as a Research Associate at the Beijing Institute of Technology working on modeling of antennas and resonators using the finite difference time domain method. From 1994 to 1997, he held the Graduate Research Assistantship with the Microwave Research Group, University of Maryland at College Park, where he worked on analysis, modeling, and design of microwave circuits and devices. Between 1994 and 1995, he also held the position of Graduate Teaching Assistant. He is now with Celwave, a division of Radio Frequency Systems, Inc. working on RF/microwave devices and systems.

Kawthar A. Zaki (SM'85–F'91) received the B.S. degree with honors from the Ain Shams University, Cairo, Egypt in 1962, and the M.S. and Ph.D. degrees from the University of California, Berkeley, in 1966 and 1969, respectively, all in electrical engineering.

From 1962 to 1964, she was a Lecturer in the Department of Electrical Engineering, Ain Shams University. From 1965 to 1969, she held the position of Research Assistant in the Electronics Research Laboratory, University of California, Berkeley. She joined the Electrical Engineering Department, University of Maryland, College Park, MD, in 1970, where she is presently a Professor of electrical engineering. Her research interests are in the areas of electromagnetics, microwave circuits, simulation, optimization, and computer-aided design of advanced microwave and millimeter wave systems and devices. She has many publications in her areas of research interests, and five patents on filters and dielectric resonators. She received several academic honors and awards for teaching, research, and inventions.